Local Feature Extraction in Fingerprints by Complex Filtering

Hartwig Fronthaler, Klaus Kollreider, and Josef Bigun

Halmstad University, SE-30118, Sweden
{hartwig.fronthaler,klaus.kollreider,josef.bigun}@ide.hh.se

Abstract. A set of local feature descriptors for fingerprints is proposed. Minutia points are detected in a novel way by complex filtering of the structure tensor, not only revealing their position but also their direction. Parabolic and linear symmetry descriptions are used to model and extract local features including ridge orientation and reliability, which can be reused in several stages of fingerprint processing. Experimental results on the proposed technique are presented.

1 Introduction

The important features of a fingerprint are divided into global and local features. Examples of global features are, e.g. singular points, around which the ridges and valleys are wrapped, ridge orientation and frequency. Local features are minutia points, which are discontinuities in the ridge flow. The most prominent minutiae are ridge bifurcation and termination (=ending), which refer to points where a ridge divides into two and a ridge ends, respectively. The estimation of ridge orientation (and frequency) is done at a scale level comparable to when detecting minutiae. For this reason we can consider ridge orientation and the reliability of its estimation as a local feature, too. In this work we extract such local features, i.e. we propose a novel method to detect the minutiae's position and direction. A topical review of fingerprint processing technologies can be found in [1]. For a description of recent techniques we refer to [2]. Existing minutia extraction approaches comprise so-called "direct grey-scale" and "binarization-based" methods. In "binarization-based" methods [3], the fingerprint image is binarized and morphologically analysed for minutiae. In "direct grey-scale" methods mainly the image gradient and local grey-scale neighbourhood are used to locate minutiae, either by tracking ridges [4], or by classifying directional filter responses [5]. The direction of the minutiae is mostly inherited from the associated ridge. The presented work can be assigned to "direct grey-scale", as it operates exclusively on the local direction field of a fingerprint image. Previously, the image is enhanced by using a contextual filtering method [6].

Complex filtering in fingerprints has recently been shown to deliver both the position and direction of singular points (of type core and delta) in a single separable filtering step [7]. Having partial fingerprints lacking singular points, only local features can be used for alignment and matching purposes. In this study

S.Z. Li et al. (Eds.): IWBRS 2005, LNCS 3781, pp. 77–84, 2005.

we present a novel way to detect the minutia points' position and direction by use of filters sensitive to parabolic and linear symmetries. The targeted minutia types are ridge bifurcation and termination. In this work, the minutiae are used for alignment (registration) of two fingerprints only. This allows us to keep the required number of minutiae low, which is advantageous when facing partial or low quality fingerprints. The fingerprint registration using minutiae is followed by a matching step employing distinctive area correlation similar to [8], except for using our features. Linear and parabolic symmetry are the only features used throughout our work.

2 Local Feature Extraction

As mentioned in [9], bifurcation and termination minutiae show (parabolic) symmetry properties similar to those of the core type singular point - but at a different scale level - thus suggesting similar extraction techniques. Linear symmetry detection is also useful for locating minutiae in an inverse fashion, as "lack of linear symmetry" occurs at minutia points [10].

2.1 Symmetry Filters

We use two types of symmetries to model and extract the local structure in a fingerprint, which are parabolic and linear symmetry. Both symmetries can be derived by separable filtering of the orientation tensor. For a more detailed review of symmetry filters, i.e. symmetry derivatives of Gaussians, we refer to [11]. Our approach starts with the orientation tensor image, described in equation (1),

$$z = (f_x + i f_y)^2 \tag{1}$$

where f_x and f_y denote the derivatives of the image in x and y direction respectively. We implement the tensor by convoluting the grey value image with separable Gaussians and their derivatives. Already the calculation of the tensor implies complex filtering since the outcome z is complex. A symmetry and the associated filter detecting it can be modelled by $\exp(im\phi)$, where m represents its order [11–13]. It was shown that an estimation for $m \geq 0$ can be done by using the following polynomial in conjunction with a Gaussian window function:

$$h_m = (x + iy)^m \cdot \exp\left(-\frac{x^2 + y^2}{2\sigma^2}\right) \tag{2}$$

First of all we are interested in parabolic symmetry of order $m = 1$, since the parabolic pattern is most similar to a minutia point in a fingerprint. Equation (3) describes how complex filtering is applied to detect this type of symmetry, where $\langle , \rangle$ represents the 2D scalar product and $g(x, y)$ denotes the Gaussian window.

$$\mathrm{PS} = \langle z, h_1 \rangle = \left\langle (f_x + i f_y)^2, (x + iy) \cdot g(x, y) \right\rangle \tag{3}$$

The two grey-scale images in figure 1 show minutia points of type ridge bifurcation (left) and ridge ending (right), with their direction indicated. Furthermore,

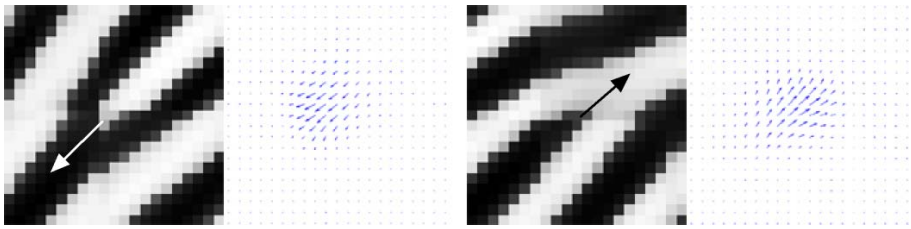

Fig. 1. Left: ridge bifurcation and filter response; Right: ridge ending and filter response

the corresponding complex filter responses of h_1 are displayed. The latter can be described as $c_1 = \mu \cdot \exp(i\alpha)$. The value μ is a certainty measure and the argument α represents the geometric orientation of the symmetric pattern in order $m = 1$. An important property of parabolic symmetry filtering for minutia detection is that the minutia direction is retrieved at the same time (see figure 1). We wish to stress that the estimated minutia direction is independent from the associated ridge.

The second type of symmetry used in this work is linear symmetry, which occurs at points of coherent ridge flow. The discrimination power of this information has been shown in fingerprint pattern matching [14]. In the case of linear symmetry, which can also be described as symmetry of order $m = 0$ the polynomial in equation (2) reduces to a Gaussian filter. Applying this filter to the orientation tensor $z(x, y)$ corresponds to summing up the local neighbourhood in each point. In order to have a reliable measure for the linear symmetry, we first calculate the second order complex moments $I_{20} = \langle z, h_0 \rangle$ and $I_{11} = \langle |z|, h_0 \rangle$, as suggested by[15, 16]. The measure for linear symmetry used in this work is denoted in equation (4).

$$\mathrm{LS} = \left(\frac{I_{20}}{I_{11}} \right) = \frac{\langle z, h_0 \rangle}{\langle |z|, h_0 \rangle} \tag{4}$$

I_{11} acts as an upper boundary for the linear symmetry certainty, and by dividing I_{20} through I_{11} unreliable orientations are attenuated, whereas the strong ones are promoted.

2.2 Detection Process

After the image enhancement and the calculation of linear and parabolic symmetry, some more steps have to be considered in order to reliably detect minutia points. First, the selectivity of the parabolic symmetry filter responses is improved, using the following inhibition scheme [17]:

$$\mathrm{PSi} = \mathrm{PS} \cdot (1 - |\mathrm{LS}|) \tag{5}$$

Essentially, in equation (5), the parabolic symmetry is attenuated if the linear symmetry is high, whereas it is preserved in the opposite case. In figure 2 the

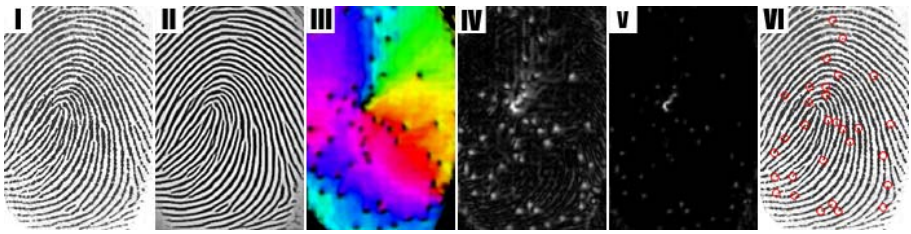

Fig. 2. Minutia point detection process

minutia detection process is visualized. The first two images visualize the initial fingerprint and its enhanced version respectively. The parabolic symmetry displayed in image IV (|PS|) is inhibited with the absolute value of the linear symmetry shown in image III (LS). The latter image also represents the local orientation. The resulting sharpened magnitudes |PSi| are displayed in image V. In a further step all filter responses below a certain threshold $\tau_{\text{reliablePS}}$ are set to zero. LS provides a good measure for segmenting the fingerprint from the background in order to discard responses in the marginal area of the fingerprint image. The remaining filter answers, which are concentrated to pixel islands, are used for the extraction of minutia candidates. During this extraction process we search for the highest filter response in a small neighbourhood of 9x9 throughout the fingerprint area in order to avoid multiple detection of the same minutia. Finally we demand each minutia to be fully surrounded by high linear symmetry, by checking whether the average linear symmetry on a ring around a minutia candidate is above a threshold $\tau_{\text{averageLS}}$. Thus we can exclude spurious minutia points which occur at the transition from the fingerprint to the background and at impurities within the fingerprint area. If this condition is fulfilled, the position and the complex filter response are stored. The final minutia list is ordered by magnitude. In image VI of figure 2, circles indicate detected minutiae when considering only the 30 highest magnitudes.

3 Pairing of Minutiae

In order to establish correspondences between two fingerprints, we implement a local minutiae matching approach inspired by triangular matching [18]. This essentially means establishing a connected series of triangles, which are equal with respect to both fingerprints and have corresponding minutiae as their corners. From the detection process we receive a minutiae list, containing the position and direction of a fingerprint's minutiae. For each minutia, additional attributes are derived from this list, which describe the relation to all other minutiae. For two arbitrary minutiae m_i and m_j contained in a list, the following attributes are stored:

1. the distance d_{ij} $(= d_{ji})$ between the two minutiae
2. the angles α_{ij} and α_{ji}, which describe the angle of the minutiae with respect to a line between each other. Note, that all angles are signed in order to be unambiguous.

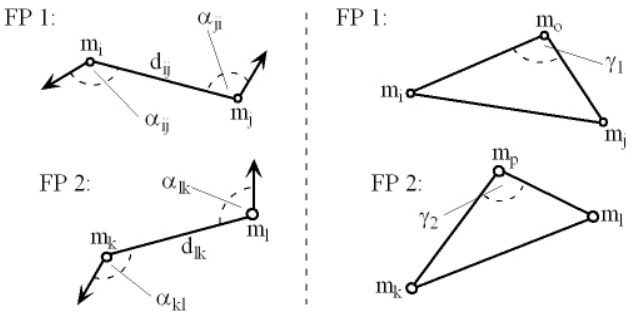

Fig. 3. Left: corresponding couples for 2 fingerprints; Right: triangles for 2 fingerprints

This is also visualized in the left part of figure 3. Having this extended minutiae list, it is possible to pre-select corresponding couples in two fingerprints, meaning two corresponding minutiae per fingerprint. Having two arbitrary minutiae m_k and m_l of a second minutiae list, the correspondence is fulfilled if $|d_{ij} - d_{kl}| < \lambda_{\text{dist}}(d_{ij})$ AND $(|\alpha_{ij} - \alpha_{kl}| + |\alpha_{ji} - \alpha_{lk}|) < \lambda_{\text{angle}}(d_{ij})$. If corresponding, the two couples are stored in a structure $C(n) = \{m_i, m_j; m_k, m_l\}$ with $n = 1..N$, where N is the number of totally found corresponding couples. The threshold functions λ_{dist} and λ_{angle} are designed to adapt to the distance between the tested minutiae. For a larger distance the angle tolerance can be decreased whereas the distance tolerance must be increased. The general use of threshold boxes, whether dynamical or not, is preferable since global distortions and inexact minutia detection can occur [2, 19].

Among all corresponding couples, which cannot be assumed to be truly corresponding in a global scope, we look for those which have a minutia in common in both of the fingerprints. Thus, taking $\{m_i, m_j; m_k, m_l\}$ as a reference, it may be that $\{m_i, m_o; m_k, m_p\}$ and $\{m_j, m_o; m_l, m_p\}$ are corresponding couples and therefore contained in C, too (i,j,o and k,l,p are minutia indices of two fingerprints respectively). This is also visualized to the right in figure 3. This constellation would imply that m_o and m_p constituted neighbours to the reference couples $\{m_i, m_j\}$ and $\{m_k, m_l\}$ respectively. To verify neighbours, we additionally demand the closing angles γ_1 and γ_2 (see figure) to be similar, which means $|\gamma_1 - \gamma_2| < \lambda_{\text{closingAngle}}(d_{io} + d_{oj})$. The latter threshold is decreasing with distance and is generally stricter than any other threshold. In this way neighbours are consecutively assigned to a reference corresponding couple, the equivalent of establishing equal triangles with respect to both fingerprints sharing a common side. Each corresponding couple is taken as a reference once. The corresponding couple, to which most neighbours can be found, is considered for further purposes. It would also be possible to cancel the search, as soon as a minimum number of neighbours was reached. Note, that the remaining triangle corners on the right hand side of figure 3 can immediately be considered and verified as neighbours to the opposite couples as well. At last the couples (one of each fingerprint) having the best correspondence are stored in a pairing list followed by their mated neighbours. This list simply links minutiae indices between the two fingerprints, e.g. $\{i, k\}$, $\{j, l\}$, $\{o, p\}$, etc.

4 Fingerprint Alignment and Matching

We assume the alignment to be a rigid transformation, since we only consider translation and rotation. The determination of the translation and rotation parameter Δx, Δy and $\Delta\phi$ is explained by means of an example using only four established minutia pairs between two fingerprints. From the paired minutia indices, we derive a list $\{A_1, A_2\}$, $\{B_1, B_2\}$, $\{C_1, C_2\}$ and $\{D_1, D_2\}$, linking the spatial coordinates of corresponding minutiae. Note, that the subscripts are used to distinguish between the two fingerprints, and each capital letter is enclosing 2D coordinates. The translation parameter is calculated by $[\Delta x\ \Delta y] = \overrightarrow{A_1 A_2}$ using the first minutia pair only. The rotation angle is determined by calculating the angle difference of two vectors between corresponding minutiae in both fingerprint parts. In order to increase the precision of the final rotation parameter $\Delta\phi$, several rotation angles are calculated and averaged. In our example $\Delta\phi$ is determined by $\Delta\phi = (\measuredangle(\overrightarrow{A_1B_1}, \overrightarrow{A_2B_2}) + \measuredangle(\overrightarrow{A_1C_1}, \overrightarrow{A_2C_2}) + \measuredangle(\overrightarrow{A_1D_1}, \overrightarrow{A_2D_2}))/3$. Furthermore we calculate the mean value m and the standard deviation σ and exclude all angles, which are not in $m \pm 0.5\sigma$ to minimize the error. It is worth mentioning that no further fine alignment is performed. Having the translation parameters and using A_2 as rotation centre, the actual alignment is straight forward [20].

After the registration of two fingerprints a simple matching using correlation can be done. Therefore we extract small areas from LS around the detected minutia points in the first fingerprint and calculate the normalised correlation with areas at the same positions in the second fingerprint. Only areas containing well-defined fingerprint regions, having an average linear symmetry higher than $\tau_{\text{averageLS}}$ are considered for matching. In order to determine the final matching score, we calculate the mean value of the single similarity scores.

5 Experiments

We present the combined performance of fingerprint alignment using our minutiae detection and pairing method, and fingerprint matching using feature correlation. For our experiments we employ the FVC2000 DB2 database (set A), which contains 800 fingerprints (100 persons à 8 fingerprints).

We carry out a fingerprint verification using the whole database. The number of impostor trials is 4950, whereas it is 2800 for the genuine trials. The maximum number of minutiae to detect in either of the fingerprints was set to 25, the size of one correlation area in the matching step was 51x51. The results are shown as a pair of FAR (False Acceptance Rate) and FRR (False Rejection Rate) curves in figure 4. The achieved EER (equal error rate) is 4.7%, also indicated by the curves' intersection point (y coordinate) in figure 4. Although not used for fingerprint matching purposes, the number of paired minutiae per trial were recorded. On the average, 11 ± 4 pairs were established in genuine trials, whereas 3 ± 1 pairs were found in the impostor trials.

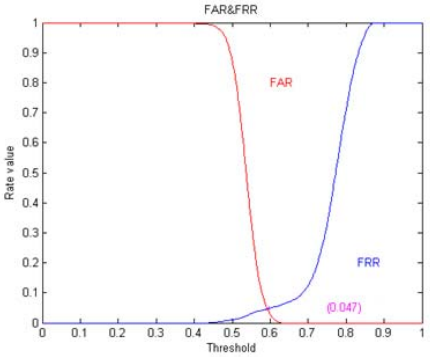

Fig. 4. FAR and FRR curves of the fingerprint verification test

6 Discussion and Conclusions

Symmetry descriptions to model and extract local features in fingerprints have been proposed in this work. Their application in several stages of a fingerprint recognition system has been shown to be efficient. In particular, the proposed minutiae detection method is novel, fast and direction aware. The minutia pairing is done intuitively and yields high accuracy enabling the fingerprint alignment. The average number of minutiae pairs established in the test trials supports the conclusion that the method can be included as an independent expert completing other experts, e.g experts using singular values, or experts matching directional maps, since efficient complementariness is increasingly being used as an argument when fusing experts and sensors in multimodal biometrics [21]. For this purpose, fingerprint distortions have to be studied further. The implemented alignment based on minutiae is not dependent either on any global features or on the size of available fingerprint area. The matching stage is able to discard unreliable fingerprint regions from the score decision. The overall performance with an achieved EER of 4.7% on a challenging database is encouraging.

Acknowledgement

The authors would like to thank Biosecure NoE IST-2002-507634 for financing this work.

References

1. Jain, A.K., Pankanti, S., Brabhakar, S., Ross, A.: Recent advances in fingerprint verification. In: Audio and Video-Based Biometric Person Authentication, Springer Ver. LNCS 2091; J. Bigun and F. Smeraldi, Eds. (2001) 182–191
2. Maltoni, D., Maio, D., Jain, A.K., Prabhakar, S.: Handbook of fingerprint recognition. (2003) Includes DVD-ROM.
3. Jain, A., Hong, L., Bolle, R.: On-line fingerprint verification. IEEE-PAMI **19** (1997) 302–314

4. Maio, D., Maltoni, D.: Direct gray-scale minutiae detection in fingerprints. IEEE-PAMI **19** (1997) 27–40
5. Leung, M.T., Engeler, W., Frank, P.: Fingerprint image processing using neural networks. In: Computer and Communication Systems. (1990) 582–586
6. Chikkerur, S., Wu, C., Govindaraju, V.: A systematic approach for feature extraction in fingerprint images. In: International Conference on Bioinformatics and its Applications. (2004) 344–350
7. Nilsson, K., Bigun, J.: Localization of corresponding points in fingerprints by complex filtering. Pattern Recognition Letters **24** (2003) 2135–2144
8. Nandakumar, K., Jain, A.K.: Local correlation-based fingerprint matching. In: Proc. of Indian Conference on Computer Vision, Graphics and Image Processing. (2004) 503–508
9. Nilsson, K.: Symmetry Filters Applied to Fingerprints. PhD thesis, Chalmers University of Technology, Sweden, Chalmers SE-412 96 Göteborg, Sweden (2005) Dissertation No 2290, ISBN 91-7291-608-7.
10. Nilsson, K., Bigun, J.: Using linear symmetry features as a pre-procesing step for fingerprint images. In Bigun, J., Smeraldi, F., eds.: Audio and Video based Person Authentication - AVBPA 2001, Springer (2001) 247–252
11. Bigun, J., Bigun, T., Nilsson, K.: Recognition by symmetry derivatives and the generalized structure tensor. IEEE-PAMI **26** (2004) 1590–1605
12. Bigun, J.: Recognition of local symmetries in gray value images by harmonic functions. In: Ninth International Conference on Pattern Recognition, Rome, IEEE Computer Society Press (1988) 345–347
13. Knutsson, H., Hedlund, M., Granlund, G.H.: Apparatus for determining the degree of consistency of a feature in a region of an image that is divided into discrete picture elements. In: US. patent, 4.747.152. (1988)
14. Bigun, J., Fronthaler, H., Kollreider, K.: Assuring liveness in biometric identity authentication by real-time face tracking. In: CIHSPS2004 - IEEE International Conference on Computational Intelligence for Homeland Security and Personal Safety, Venice, Italy, IEEE Catalog No. 04EX815, ISBN 0-7803-8381-8 (2004) 104–112
15. Bigun, J., Granlund, G.H.: Optimal orientation detection of linear symmetry. In: First International Conference on Computer Vision, ICCV, June 8–11, London, IEEE Computer Society Press, Washington, DC. (1987) 433–438
16. Kass, M., Witkin, A.: Analyzing oriented patterns. Computer Vision, Graphics, and Image Processing **37** (1987) 362–385
17. Johansson, B.: Multiscale curvature detection in computer vision. Lic. thesis no. 877; LIU-TEK-LIC-2001:14, Linkoping University, Dep. EE (ISY), SE-581 83, Linkoping (2001)
18. Kovacs-Vajna, Z.: A fingerprint verification system based on triangular matching and dynamic time warping. IEEE Transactions on Pattern Analysis and Machine Intelligence **22** (2000) 1266–1276
19. Jea, T., Govindaraju, V.: A minutia-based partial fingerprint recognition system. The Journal of Pattern Recognition (2005)
20. Wilkinson, F., Wilson, H.R., Habak, C.: Alignment using distributions of local geometric properties. IEEE Trans. Pattern Analysis and Machine Intelligence **21** (1999) 1031–1043
21. Fierrez-Aguilar, J., Nanni, L., Ortega-Garcia, J., Cappelli, R., Maltoni, D.: Combining multiple matchers for fingerprint verification: a case study in fvc2004. In: Proc. of 13th IAPR Intl. Conf. on Image Analysis and Processing, Cagliari, Italy. Volume LNCS-3617., Springer (2005) 1035–1042